RESEARCH ARTICLE

Conjugated Polymer Nanotherapeutics for Next Generation Photodynamic Therapy

Authors

Andre J. Gesquiere[*,1,2,3,4], Khalaf Jasim[1,2], Martin Topps[1,2], Sajan Shroff[5], Alondra M. Ortiz Ortiz[6], Olivia George[7], Yasmine Abdellatif[1]

Affiliations:

[1]NanoScience Technology Center, University of Central Florida, Orlando, FL 32826, USA
[2]Department of Chemistry, University of Central Florida, Orlando, FL 32816, USA
[3]Department of Materials Science and Engineering, University of Central Florida, Orlando, FL 32816, USA
[4]The College of Optics and Photonics (CREOL), University of Central Florida, Orlando, FL 32816, USA
[5]Windermere Preparatory School, Windermere, FL 34786, USA,
[6]Department of Mechanical Engineering, University of Puerto Rico, Mayaguez Campus, Mayaguez 00681-9000, Puerto Rico,
[7]Department of Chemical Engineering, University of Tennessee at Chattanooga, Chattanooga, TN 37403, Tennessee

Correspondence

A.J. Gesquiere
E-mail: andre@ucf.edu

Abstract

First and second-generation photosensitizers for Photodynamic Therapy (PDT) are in clinical trials, with a few approved for clinical application. While effective, several drawbacks have remained unaddressed that could increase the impact of PDT as an efficient therapy, including lack of selectivity to diseased tissue, toxicity, low to moderate light absorption, and poor solubility of the sensitizers that results in low bioavailability. It's likely that a new generation of PDT sensitizers must be developed to improve on these shortcomings.

In this review, we summarize our progress in the development of Conjugated Polymer Nanoparticles as a next generation nanotherapeutic for Photodynamic Therapy. We show that their unprecedented light absorption, efficient ROS generation, high level of targeted delivery and selective uptake, absence of dark toxicity and high percentage of PDT induced cell mortality observed indicate a promising next generation PDT sensitizer. The simple design and ease of fabrication of the Conjugated Polymer Nanoparticles holds promise for broad applicability.

1. Introduction

Chemotherapy [1-5], surgery [6-8] and radiotherapy [9,10] are currently widely used in clinical settings for melanoma treatment. Surgery has recently seen improvements by the development of laser surgery [11-15] and fluorescence imaging guided surgery [16,17]. Promising new anticancer drugs such as doxorubicin [18-20] have been extensively studied, and STAT3 inhibitors [21-23] are currently under investigation. Nanotechnology based formulations have also shown promise with their improved delivery and therapeutic properties.[24,25] Photodynamic Therapy (PDT) has been shown to be a promising treatment scheme for specific tumor types through clinical trials and application at treatment centers [26-31]. Despite these advances, many cancers appear with challenges such as genetic diversity, drug resistance, and patient remission. In addition, drug delivery, drug effectiveness, and site specificity of treatments remain major challenges in the development of treatment strategies.

For cancers in tissues that are accessible without invasive surgery, Photodynamic Therapy (PDT) does provide an avenue as an adjuvant therapy to increase effectiveness of current leading treatment methods. In particular, it has been recently shown that PDT can elicit an antitumor immune response.[32] Photodynamic Therapy (PDT) can be also highly suitable for Stage II and Stage III cancers, where tumors have developed and metastasis to nearby lymph nodes may have occurred. In PDT a photosensitizer is administered to tissue and irradiated with visible light matching to the absorption spectrum of the photosensitizer.[25,32] The photosensitizer produces Reactive Oxygen Species (ROS), highly reactive forms of oxygen, which can result in cell mortality.[33-35] PDT does, however, present problems with sensitizer solubility (most are hydrophobic and not compatible with physiological conditions), side effects and non-specific interactions with tissue due to broad distribution of the photosensitizer in the body, low to moderate light absorption (the best sensitizers such as Phthalocyanines, Porphyrines, and Photofrin (which is a Porphyrin) have extinction coefficients [ε] of several 10^{-5} L mol^{-1} cm^{-1} at best), and low accumulation at the tumor site.[36-42] These limitations require administering large doses of sensitizer, which then requires patients to avoid sunlight for four to six weeks after treatment. PDT with drastically improved sensitizers including better light absorption, better dispersibility in biologically relevant media and controlled delivery to tumors has the potential to advance PDT as an approach in a combinatorial or independent treatment scheme.

Some answers can be found in the development of nanotechnology enabled platforms, in particular for improvement of sensitizer dispersibility and controlled delivery. A number of inorganic nanoparticle photosensitizers including quantum dots,[43,44] gold nanoparticles,[45-47] magnetic nanoparticles,[48,49], and metal-oxide nanoparticles[50-54] are under study. Organic platforms have also been developed to encapsulate or envelop PDT sensitizers.[55-60]

Recently, photosensitizer-doped conjugated polymer nanoparticles have received attention as potential photosensitizers for PDT. McNeill et al. developed conjugated polymer nanoparticles (CPNPs) with the photosensitizer blended into the nanoparticle.[61] They observed singlet oxygen formation from the tetraphenylporphyrine (TPP) photosensitizer embedded in the CPNPs and DNA damage under PDT conditions.[61] The Xu and Saeed groups followed up with reports on

PDT with similar CPNPs showing singlet oxygen luminescence [62] and PDT effects [63]. Further progress has been reported in the development of doped, multifunctional and near-infrared absorbing CPNPs recently by several groups.[64-70]

Our group has published extensively on the fabrication of conjugated polymer nanoparticles (CPNPs) such as those obtained from poly[2-methoxy-5-(2-ethylhexyl-oxy)-p-phenylenevinylene] (MEH-PPV).[71-76] Here we review our work showing the success of the CPNPs *in vitro* for PDT application including for targeted delivery and therapeutics. The significance of CPNPs as next generation sensitizers for PDT compared to existing sensitizers lies in their (i) large extinction coefficients ($\varepsilon > 10^7$ L mol^{-1} cm^{-1}, i.e. 2 to 3 orders of magnitude higher than current small molecule sensitizers such as Phthalocyanine, Porphyrin, and Photofrin), (ii) efficient triplet formation as necessary for PDT with triplet energies that are close to that of oxygen,[77] (iii) intrinsic ROS formation (no need for sensitizing dopants or encapsulation of conventional sensitizers), (iv) low to absent cytotoxicity found *in vitro* (in dark), (v) buffer dispersibility and stability, (vi) intrinsic fluorescence for tracking of delivery (no need for dye dopant or attachment), and (vii) adaptable design for targeted delivery. The large extinction coefficient ε indicates that the photon absorption rate is 2 to 3 orders of magnitude higher than current small molecule sensitizers (where the best sensitizers have an extinction coefficient of several 10^{-5}). Thus, the resulting rate of ROS generation for PDT is 2 to 3 orders of magnitude higher for our CPNPs compared to current small molecule sensitizers, and CPNPs could generate therapeutic doses of ROS with 100 to 1,000 times less light exposure. *In vivo* studies by McNeill et al. have shown that such CPNPs are able to circulate in the body and reach tumor tissue without direct injection into the tumor, further indicating their usefulness as next generation PDT photosensitizers.[78]

2. Non-tumor targeted conjugated polymer nanoparticles

In this section, we present progess made in developing MEH-PPV based CPNPs with respect to the use of the photosenstizing dopant phenyl-C61-butyric acid methyl ester (PCBM) (Figure 1)

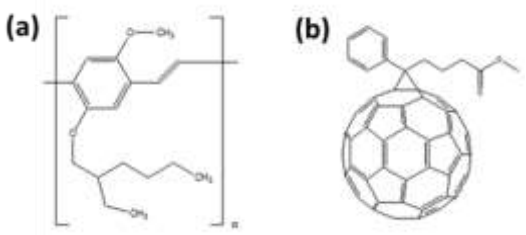

Figure 1: Schematic of the (a) poly[2-methoxy-5-(2-ethylhexyl-oxy)-p-phenylenevinylene] (MEH-PPV) and (b) phenyl-C61-butyric acid methyl ester (PCBM).

The design of these CPNPs is based on efficient charge transfer between MEH-PPV and PCBM that enhances formation of radicals.[79] These radicals then further enhance ROS formation in the presence of oxygen. Fullerene has shown successful application in PDT applications in both dispersed molecular form as well as in fullerene nanoparticles.[80-85] Limitations were found, however, with cytotoxicity of

these materials.[84] The benefit of blending the fullerene PCBM into composite MEH-PPB/PCBM CPNPs is that fullerene cytotoxicity is substantially reduced. We also show in this section that although adding a sensitizing dopant does have some benefits in increasing PDT effectiveness, the gains may not be sufficient to warrant the extra steps in preparation or risks of introducing cytotoxicity in the CPNP design. Indeed, the conjugated polymer that forms CPNPs is a highly effective PDT sensitizer itself.

2.1 Fullerene doped MEH-PPV CPNPs as PDT sensitizers

The MEH-PPV/PCBM CPNPs were prepared by the reprecipitation method.[76] This method produces CPNPs in ∼20–100 nm size range,[76] which is ideal for internalization by cells.[86-88] We settled on 50 wt% PCBM doping level since this blend affords efficient charge transfer between MEH-PPV and PCBM, with a quantum efficiency that is near 1.[89] To evaluate the intrinsic (i.e. in the absence of light exposure for PDT) cytotoxicity of the MEH-PPV/PCBM CPNPs we used the MTT *in vitro* assay to quantify cell proliferation properties in the presence and absence of CPNPs.

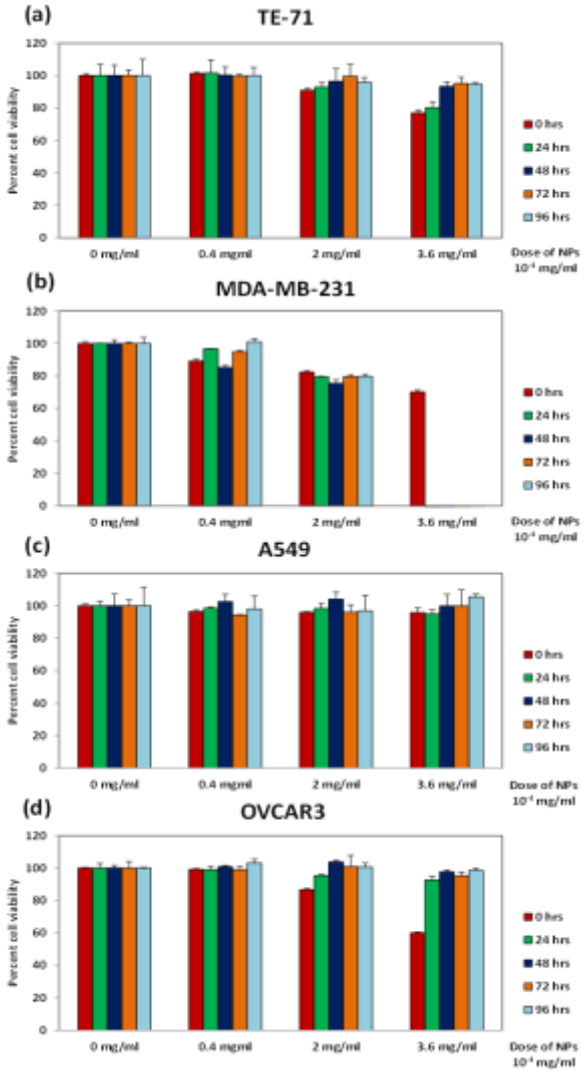

Figure 2: Normalized cell viaability for cell lines dosed with MEH-PPV/PCBM CPNPs under dark conditions (no PDT applied), compared with the control (no CPNPs). Reprinted from Ref. [90] with permission from Springer.

Our data, presented in Figure 2, show that the CPNPs do not affect the proliferation of the cell lines used in the study, except for the breast cancer cell line (MDA-MB-231) at the highest applied dose of CPNPs, where the cell population dies off instead of proliferating normally. The mechanisms that make the breast cancer cell line unusually sensitive to the MEH-PPV/PCBM CPNPs are curently not understood. The quenching of MEH-PPV fluorescence due to the presence of PCBM made quantification of CPNP internalization by flow cytometry problematic, but overall CPNP internalization was observed with confocal microsocpy (data not shown) to scale with aggresiveness of the cancer type, with the OVCAR3 ovarian cancer cell line being the most aggressive.[91,92]

The MTT *in vitro* assay was also used to determine effectiveness of PDT with MEH-PPV/PCBM CPNPs. Three CPNP doses were evaluated. Immediately after PDT the MTT assay shows effectiveness of the *in*

vitro PDT treatment. Our data indicate that immediately following PDT the live cell population for the TE-71 control cell line is reduced by nearly 20 %, MDA-MB-231 shows decreases approaching 30%, for A549 decreases approaching 40 % are observed, and for OVCAR3 up to 70 % reduction in cell population is observed immediately after PDT. We also left the samples in the incubator for 4 and 12 hours after PDT treatment to determine if there are any delayed effects for treatment to be effective, for instance due to persistence of ROS. The data for the 4 hour time point is shown in Figure 3. At the 4 hours post-PDT incubation time point the live cell population for the TE-71 control cell line was found to be consistent at 20% population reduction, MDA-MB-231 showed an additional 5% decreases, A549 population decrease jumped to 60%, and for OVCAR3 a near complete reduction in cell population was observed for the 2×10^{-4} and 3.6×10^{-4} mg/ml CPNP doses at light doses >60 J/cm^2. The 12 hour time point provided no significant improvement over the 4 hour time point results. Phototoxicity controls (*vide infra*, no CPNPs, exposure to highest light dose) show no cell death upon light exposure, so the observed decreases in cell viability confirm that CPNPs taken up by cell lines (including the non-cancer control) are PDT active.

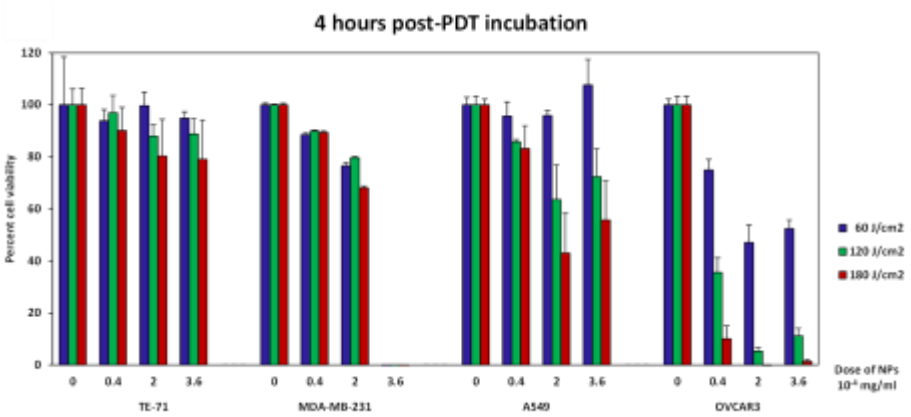

Figure 3: MTT cell viability assays 4 hours after completion of composite MEHPPV/PCBM-based PDT. PDT using three CPNP doses and three light doses was studied. Adapted from Ref. [90] with permission from Springer.

The PDT data suggest modest "passive" targeting of the MEH-PPV/PCBM CPNPs to cancer lines compared to the non-cancer control, which could be due to differences in surface charge on the cell membrane of the different cell lines. Reports indicate that cancer cell lines have less negative charge on their surfaces compared to normal cell lines,[93] which allows NPs (average zeta potential is −9.66±8.1 mV) to have more interaction with cancer cells than with the normal cells.[94-96] Differences in metabolic rate (aggressiveness) between the normal cell line and the cancer cell lines should also be considered.[91,97-99]

Comparing the results among the cancer cell lines, the substantially greater effectiveness towards the ovarian cancer cell line is probably related to the higher metabolic rate (aggressiveness) of this cancer type and differences in internalization pathways between cancer cell lines. Published literature gives a strong indication that the OVCAR3 cell line is more aggressive than the MDA-MB-231 breast cancer or A549 lung cancer cell

lines.[91,92] It is also important to consider differences in CPNP internalization pathways across these cell lines. Our study on CPNP internalization suggests Caveolae-Mediated Endocytosis as a primary uptake mechanism in the case of HeLa cells (human epithelial carcinoma cell line),[100] but in broader context clathrin- and claveolae-mediated endocytosis, and (macro)pinocytosis require consideration for nanoparticle internalization.[43] For instance, it has been shown that for A549 nanoparticles are internalized exclusively by clathrin-mediated endocytosis,[101] while for OVCAR3 nanoparticles go through energy-dependent uptake pathways,[102] which are all of the pathways discussed above. It's thus possible to speculate that the high CPNP uptake by OVCAR3 is due to the involvement of all these pathways compared to the single nanoparticle internalization pathways available for A549 and MDA-MB-231.

To learn more about the CPNP induced PDT effect a double staining live/dead imaging experiment was completed. Interestingly, as shown in Figure 4, we find that for OVCAR-3 apoptotic cell death occurs followed by necrosis at the lower PDT light doses. A549 only exhibits necrosis. It's likely though that adjusting CPNP or light dose could also prompt an apoptotic response from A549. The observation of apoptotic cell death upon CPNP PDT is interesting in that it that it gives potential to elicit an antitumor immune response.[32]

Overall, the MEH-PPV/PCBM CPNPs show unexpected specificity towards certain cancer cells, yield highly effective PDT treatment, and are able to induce apoptosis in human ovarian cancer (OVCAR3) *in vitro*.

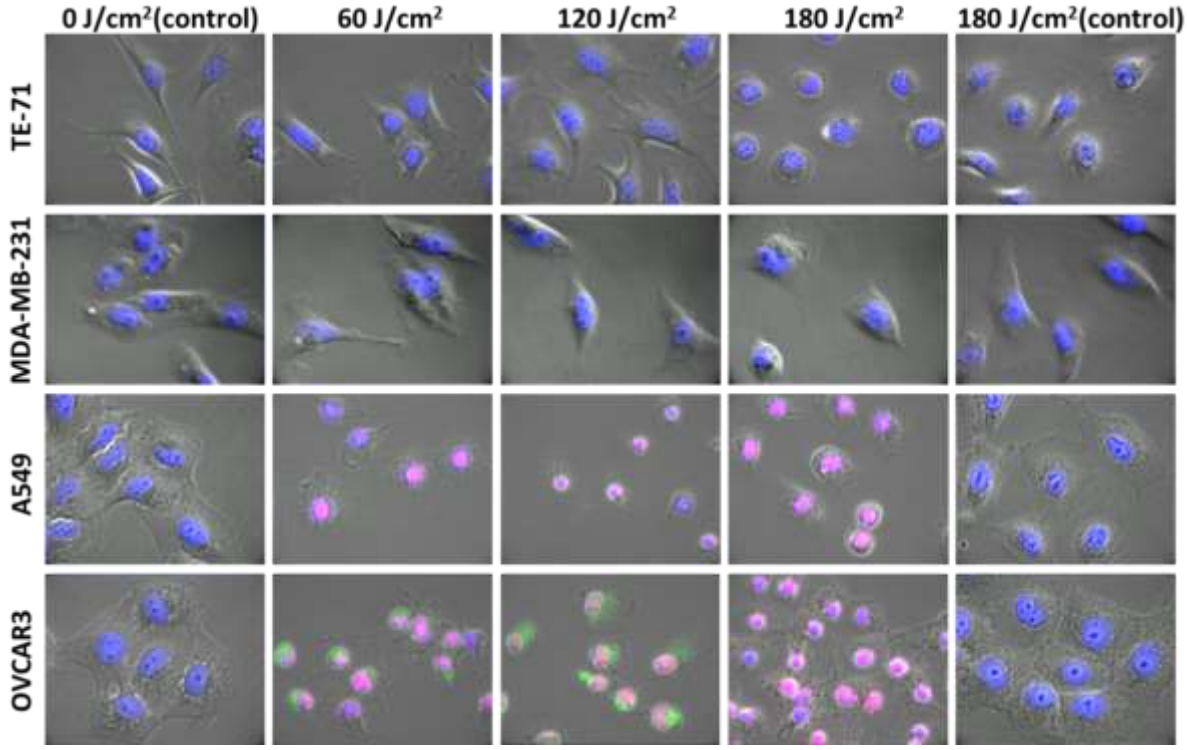

Figure 4: Live/dead staining and fluorescence imaging for observation of apoptotic (FITC-annexin V, green) and necrotic cell (PI, red) death from PDT using composite MEH-PPV/PCBM CPNPs. Reprinted from Ref. [90] with permission from Springer.

2.2 Undoped MEH-PPV CPNPs as PDT sensitizers

When considering potential clinical applicability, it's important to keep therapeutic designs simple and avoid designs that jeopardize regulatory approval. The MEH-PPV/PCBM CPNPs reviewed in section 2.1 show great performance and usefulness in PDT, but the presence of the fullerene and the observation of cytotoxicity for the MDA-MB-231 cell line raises questions about their chances to make it to clinical application. We therefore continued by investigating the intrinsic PDT properties of MEH-PPV CPNPs without addition of further sensitizers.

The approach was deemed feasible because MEH-PPV is efficient at triplet formation, with triplet energies that are close to that of oxygen (as necessary for PDT).[77] MEH-PPV was thus expected to sensitize ROS formation without further addition of sensitizing dopants. As expected, signs of cytoxicity observed for MEH-PPV/PCBM CPNPs were not observed for MEH-PPV-only CPNPs (data not shown). All cell lines studied showed populations that were not significantly different from the control (no CPNP). In addition, without PCBM present the MEH-PPV CPNPs are brightly fluorescent. Their fluorescence signal was used to quantify internalization of the non-tumor targeted MEH-PPV CPNPs by flow cytometry, see Figure 5.

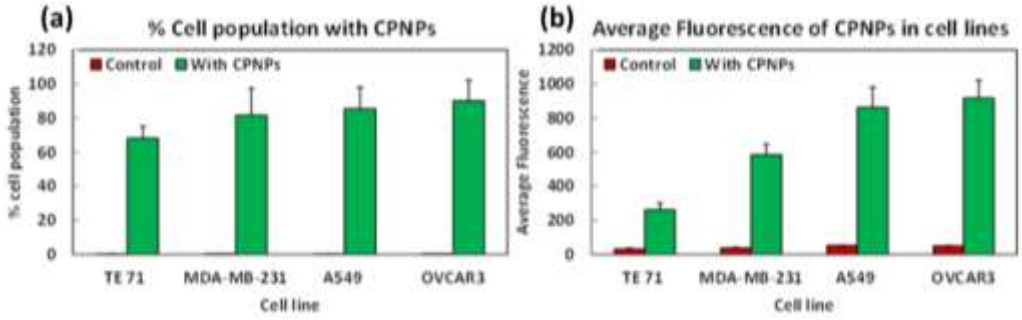

Figure 5: Flow cytometry data plotted to show (a) percentage of the cell population that internalized CPNPs (green bars) together with controls (red bars, no CPNPs), and (b) average fluorescence intensity observed from CPNPs (green bars) together with controls (red bars, no CPNPs). Adapted from Ref. [103] with permission from Elsevier.

CPNP internalization shows the same trend as discussed for the MEH-PPV/PCBM CPNPs, quantitatively confirming the arguments made in section 2.1. Flow cytometry data summarized in Figure 5 (a) shows that 68.2% of TE-71 cells internalized CPNPs, and 81.6%, 85.6%, and 90.05% of cells internalized CPNPs for MDAMB-231, A549, and OVCAR3, respectively. If we also consider the average fluorescence intensity of CPNPs in each cell line, shown in Figure 5 (b), a clear distinction between amount of cells with CPNPs and amount of CPNPs per cell can be made. Specifically, while an apparently large population of the non-cancer control cell line (TE71) internalized CPNP, the amount internalized is much less than CPNPs internalized by the cancer cell lines.

These findings were corroborated by confocal fluorescence imaging, for which the images shown in Figure 6 clearly illustrate the trend in CPNP internalization. CPNPs are abundant inside OVCAR3 and show least internalization by TE71. The CPNPs appear to lozalize in the cytoplasm.

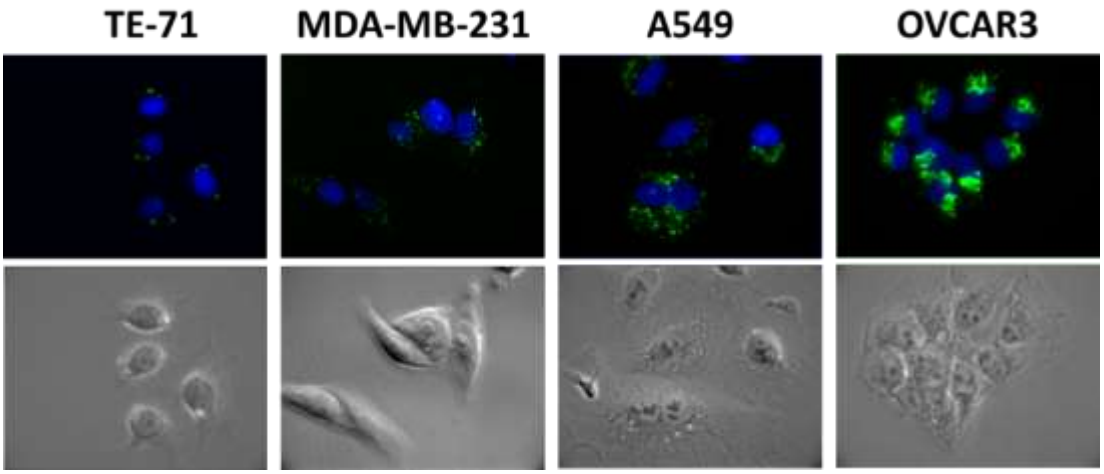

Figure 6: Confocal fluorescence images and phase contrast images of TE-71, MDA-MB-231, A549 and OVCAR3 cells. The cells were incubated with $3.6*10^{-4}$ mg/ml MEH-PPV CPNPs. The green color shows the fluorescence detected from the CPNPs. Nuclei were stained with DAPI (blue). Adapted from Ref. [103] with permission from Elsevier.

For PDT experiments the cell lines were incubated with three different doses of MEH-PPV CPNPs (0.4×10^{-4} mg/ml, 2×10^{-4} mg/ml and 3.6×10^{-4} mg/ml) and exposed to three different light doses (60 J/cm^2, 120 J/cm^2 or 180 J/cm^2). No phototoxicity was found during the experiments. PDT effectiveness was determined by MTT assay immediately after the treatment (data not shown), and after a post PDT incubation period of 4 h (Figure 7) and 12 h in dark (data not shown).

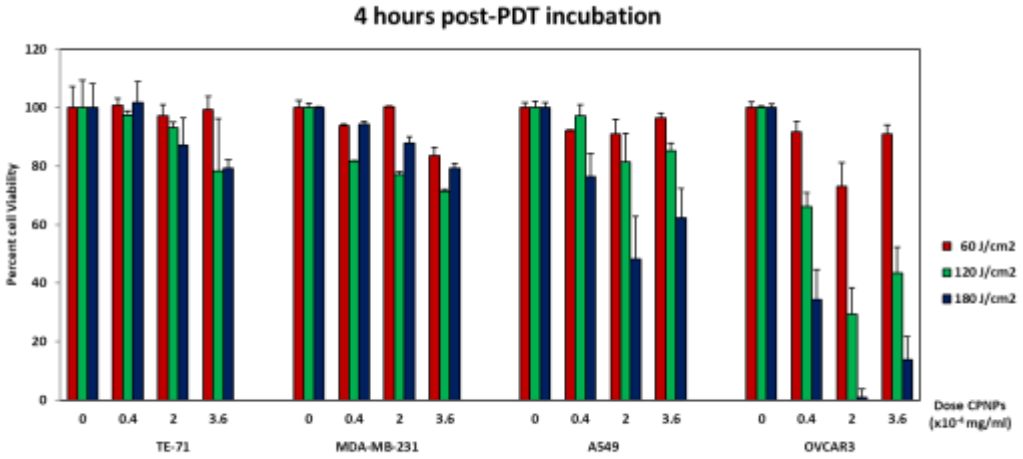

Figure 7: Cell populations determined by MTT assay after PDT treatment with different MEH-PPV CPNP doses and different light doses. Adapted from Ref. [103] with permission from Elsevier.

For each experiment, the cell population decreases from TE-71, MDA-MB-231, and A549 to OVCAR3, consistent with how MEH-PPV CPNP internalization varied. Looking at the individual cancer cell lines the cell population decreases with increasing CPNP dose. At the highest dose (3.6×10^{-4} mg/ml) a plateau in effectiveness appears to be reached. The non-cancer control cell line (TE71) shows no significant CPNP dose response due to the limited CPNP uptake. Light dose dependence is observed for A549 and OVCAR3. The higher amount of CPNPs uptaken by cells lines such as A549 and OVCAR3 compared to MDA-MB-231 leads to higher amounts of ROS and increased cell death as a result. Similar to the MEH-PPV/PCBM CPNPs, after 4 hours post-PDT incubation the highest cell death was recorded and the 12 hour time point provided no significant improvement over the 4 hour time point results.

Overall, the MEH-PPV CPNPs are profusely internalized by cancer cells without surface functionalities that target specific receptors on cancer cell membranes. Modest specificity towards cancer cells was found due to the surface charge of the MEH-PPV CPNPs and the different metabolic rates that cancer cells exhibit. The bright intrinsic fluorescence of the CPNPs brings great utility in fluorescence imaging to track the CPNPs. PDT with MEH-PPV CPNP was found to be effective, and scales with the extent of CPNP uptake and administered light dose. For the OVCAR3 cell line cell viability is near zero after treatment.

3. Tumor targeted conjugated polymer nanoparticles

There is no doubt about the potential effectiveness of non-targeted PDT photosensitizers, especially if direct injection into tumor tissue is possible. However, PDT photosensitizers are mostly administered intravenously into the body, and the sensitizer circulates through the body until cleared. Patients must avoid light for several weeks to avoid toxic side effects.[104,105] Targeting the photosensitizer to the tumor tissue, where it should accumulate, can address such issue. This is frequently accomplished by decorating the nanoparticle surface with antibodies specific towards certain tumor types,[106] or with ligand molecules that target receptors overexpressed by tumors.[91,107-110]

Since MEH-PPV itself is not a good platform to perform chemistry on to introduce tumor targeting functionality on the MEH-PPV CPNP surface, we co-reprecipitated polystyrene graft ethylene oxide carboxylate (PS-PEO-COOH) with MEH-PPV during CPNP preparation.

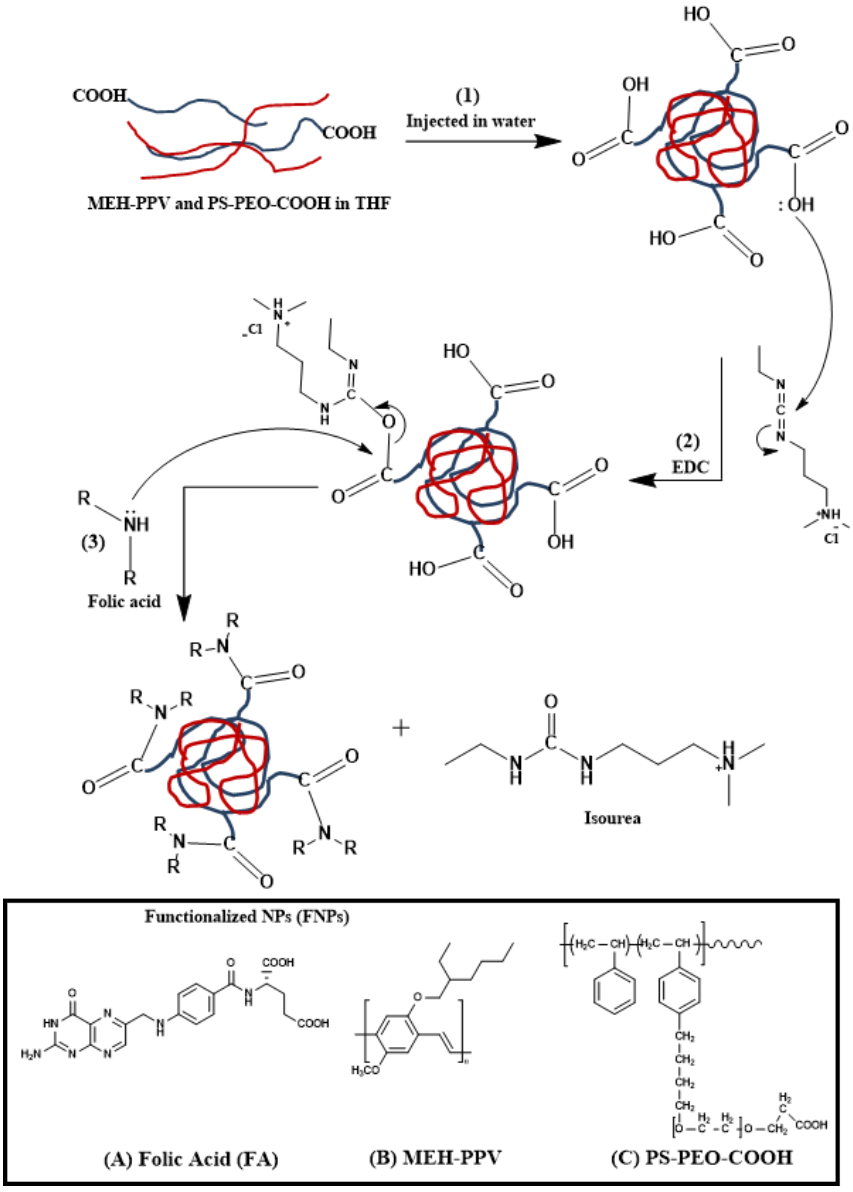

Figure 8: Schematic of the process to functionalize MEH-PPV/ PS-PEO-COOH CPNPs with folic acid. Adapted from Ref. [111] with permission from The Royal Society of Chemistry.

Since the PS-PEO-COOH carboxyl groups are hydrophylic these point to water, while the hydrophobic polystyrene graft ethylene oxide polymer chain intermingles with MEH-PPV in the CPNPs. The carboxyl groups were then used with peptide chemistry to form covalent linkages with tumor targeting ligands. We choose folic acid as the targeting ligand since OVCAR3 strongly overexpresses the folate receptor (FR+).[91,112-116] Conversely, little overexpression of the folate receptor is reported for A549.[115,117-125] The MIA PaCa-2 cell line overexpresses other receptors and is negative for the folate receptor (FR-). The protocol of folic acid attachment to the MEH-PPV/ PS-PEO-COOH CPNPs follows the typical EDC/NHS (N-(3-dimethylaminopropyl)-N0-ethylcarbodiimide hydrochloride/N-

Hydroxysuccinimide) peptide chemistry. The process is shown in Figure 8. The resulting folic acid functionalized MEH-PPV/ PS-PEO-COOH CPNPs are labeled as FNP for clarity.

The resulting FNPs remain brightly fluorescent and show no cytotoxicity (data not shown). Taking advantage of the FNP fluorescence, selectivity of FNP uptake was evaluted by flow cytometry after incubating TE71, MIA PaCa-2. A549, and OVCAR3 with 2×10^{-4} mg/ml FNPs. The applied FNP dose was informed by the work reviewed in Section 2.2.

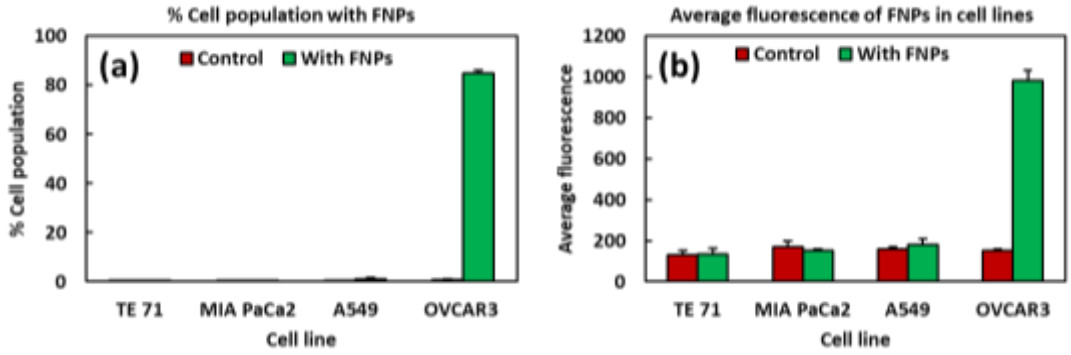

Figure 9: Uptake of FNPs quantified by flow cytometry. (a) Bar graph the percentage cell population that has internalized FNPs. (b) Bar graph indicating the average fluorescence intensity observed from FNPs for different cell lines. Red bars are data for the controls (no FNPs). Adapted from Ref. [111] with permission from The Royal Society of Chemistry.

Flow cytometry data shown in Figure 9 confirm successful targeting to the FR+ cell lines (OVCAR3) through the folic acid ligand on the FNP surface. TE 71, MIA PaCa-2 and A549 data show no significant difference with the untreated (no FNPs) control, while for the OVCAR3 cell line 85% of the cell population has internalized FNPs.

Effectiveness and targeted nature of PDT was quantified by MTS assay (Figure 10) and flow cytometry (Figure 11). The MTS assay clearly shows that only the OVCAR3 cell lines are affected by the PDT treatment. Data for the other cell lines are not significantly different from the untreated control and the non-cancer cell line, consistent with the absence of FNP internalization and highly targeted nature of the FNPs.

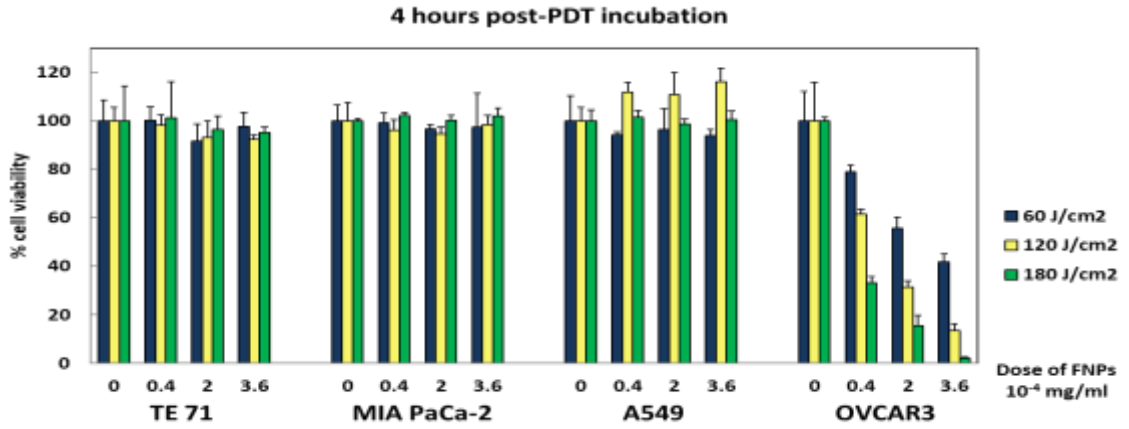

Figure 10: MTS viability assay was used to quantify the cell population of PDT treated samples with respect to untreated (no FNPs added) control. Adapted from Ref. [111] with permission from The Royal Society of Chemistry.

Flow cytometry was completed with the use of PI and Annexin V FITC staining after 4 hours of post-PDT incubation, which was previously determined to be time point where maximum PDT effectiveness is observed (see sections 2.1 and 2.2). The selected cell staining scheme allows for the evaluation of cell death efficiency and pathways. Results are shown in Figure 11. Panels A through D show 2D fluorescence intensity plots with annexin V FITC fluorescence intensity on the x-axis and PI (propidium iodide) fluorescence intensity on the y-axis. Data for untreated controls (no FNPs, stain added) are shown in red, data for treated samples (FNPs added, stain added) are shown in black.

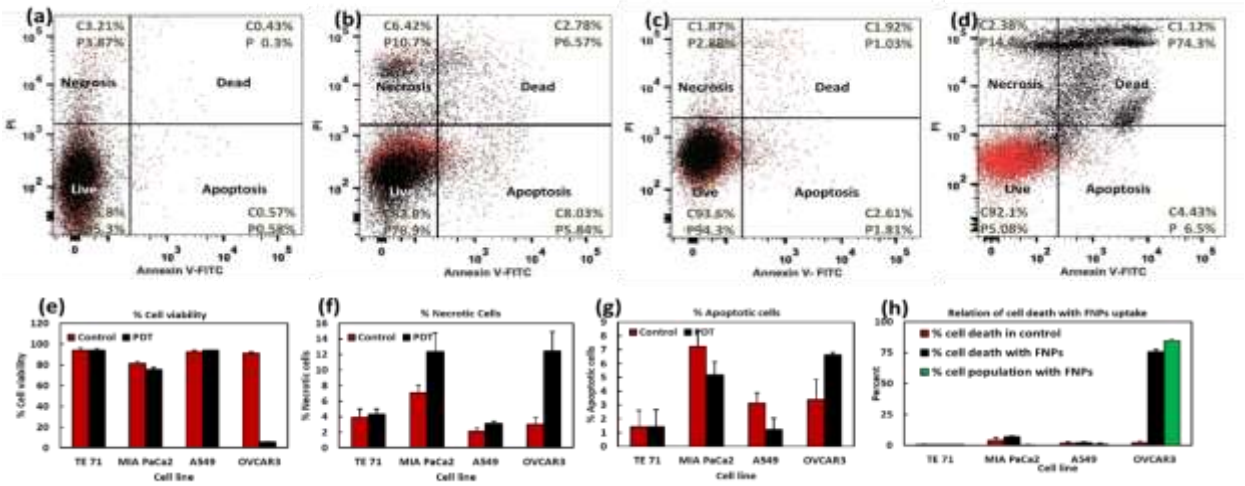

Figure 11: Flow cytometry data for PDT/FNP treated samples (black) and PDT untreated (no FNP) controls (red). 2D fluorescence dot plots for annexin V FITC and PI fluorescence are shown for (a) TE 71 (non-cancer control), (b) MIA PaCa-2 (FR-), (c) A549 (FR-) and (d) OVCAR3 (FR+). Overall cell viability (e), fraction of necrotic (f) and apoptotic cells (g), and the relation between PDT induced cell death and FNP uptake are shown as bar graphs. Adapted from Ref. [111] with permission from The Royal Society of Chemistry.

In these plots, live cells show up in the lower left quadrant, apoptotic cells in the lower right quadrant, necrotic cells in the top left quadrant, and cells that are double stained (showing both with annexin V FITC and PI fluorescence). Quantifying the results reveals that for the OVCAR3 cell line (Figure 11 (d)), almost 75% of the cells are dual stained, 14% cells are stained by PI only (necrotic) and 6% cells are stained by annexin V-FITC (apoptotic). The other cell lines are not significantly different from their controls, again consistent with the highly targeted nature of the FNPs and effective PDT on the target. We analyzed the data further to quantify overall cell viability Figure 11 (e) and its relation to FNP uptake Figure 11 (h), and fraction of necrotic Figure 11 (f) and apoptotic cells Figure 11 (g). For overall cell viability the PDT treated non-targeted cancer cell lines and the non-cancer control line are indistinguishable from the untreated (no FNP) controls. For the targeted cancer cell line, however, only 5% of cells survive treatment. Observations are consistent with the MTS assay results. From flow cytometry we also learned that the OVCAR3 cell line has 14% necrotic cells and 6.5% apoptotic cells, the rest of the dead cells are double stained. Note that some cell death (~15%) is observed for MIA PaCa-2 in both the treated sample and untreated control. We found MIA PaCa-2 to be very sensitive to handling during measurements. Finally, Figure 11 (h) indicates a 1:1 correlation between FNP uptake and PDT effectiveness for the targeted cancer cell line, OVCAR3.

Overall, the *in vitro* PDT experiments with the FNPs (MEH-PPV/PS-PEO-COOH/Folic Acid CPNPs) show almost complete cell killing for OVCAR3, the targeted cancer cell line, making the FNPs highly effective PDT sensitizers. No PDT induced cell mortality is observed for the non-targeted cell lines, indicating excellent targeting capability of the FNPs.

4. Conclusion and Outlook

Substantial progress has been made in addressing limitations of past and current generation PDT sensitizers through the development of Conjugated Polymer Nanoparticles as a next generation PDT photosensitizer. Conjugated Polymer Nanoparticles have been shown to be effective nanotherapeutics for PDT. Their unprecedented light absorption, efficient ROS generation, high level of targeted delivery and selective uptake, absence of dark toxicity and high percentage of PDT induced cell mortality observed indicate a promising next generation PDT sensitizer. Further advancements can be made by developing near-infrared absorbing CPNPs, work that is in progress in our group and at other groups, to improve their usefulness in treating tumors that are not at the surface of tissues. Futhermore, PDT requires oxygen to be present at the tumor site, however, tumors often exhibit hypoxia. This issue has remained unresolved and requires further study.

Acknowledgements

The authors would like to thank the National Science Foundation for support of this work through REU site EEC 1560007.

References

[1] Dent, S.; Oyan, B.; Honig, A.; Mano, M.; Howell, S. HER2-targeted therapy in breast cancer: A systematic review of neoadjuvant trials. *Cancer Treat. Rev.* **2013**, *39*, 622-631.

[2] Heinemann, V.; Douillard, J. Y.; Ducreux, M.; Peeters, M. Targeted therapy in metastatic colorectal cancer - An example of personalised medicine in action. *Cancer Treat. Rev.* **2013**, *39*, 592-601.

[3] Mountzios, G.; Soultati, A.; Pectasides, D.; Pectasides, E.; Dimopoulos, M. A.; Papadimitriou, C. A. Developments in the systemic treatment of metastatic cervical cancer. *Cancer Treat. Rev.* **2013**, *39*, 430-443.

[4] Verbrugghe, M.; Verhaeghe, S.; Lauwaert, K.; Beeckman, D.; Van Hecke, A. Determinants and associated factors influencing medication adherence and persistence to oral anticancer drugs: A systematic review. *Cancer Treat. Rev.* **2013**, *39*, 610-621.

[5] Xie, X.; Wang, S. S.; Wong, T. C. S.; Fung, M. C. Genistein promotes cell death of ethanol-stressed HeLa cells through the continuation of apoptosis or secondary necrosis. *Cancer Cell Int.* **2013**, *13*, 1-15.

[6] Fisher, B.; Anderson, S.; Bryant, J.; Margolese, R. G.; Deutsch, M.; Fisher, E. R.; Jeong, J.-H.; Wolmark, N. Twenty-Year Follow-up of a Randomized Trial Comparing Total Mastectomy, Lumpectomy, and Lumpectomy plus Irradiation for the Treatment of Invasive Breast Cancer. *New England Journal of Medicine* **2002**, *347*, 1233-1241.

[7] Fong, Y.; Fortner, J.; Sun, R. L.; Brennan, M. F.; Blumgart, L. H. Clinical score for predicting recurrence after hepatic resection for metastatic colorectal cancer: analysis of 1001 consecutive cases. *Annals of surgery* **1999**, *230*, 309-318; discussion 318-321.

[8] Ishitobi, M.; Suzuki, O.; Komoike, Y.; Ohsumi, S.; Nakahara, S.; Yagi, T.; Yoshinami, T.; Tomita, Y.; Inaji, H. Phase II study of neoadjuvant anastrozole and concurrent radiotherapy for postmenopausal breast cancer patients. *Breast Cancer* **2014**, *21*, 550-556.

[9] Kalbasi, A.; June, C. H.; Haas, N.; Vapiwala, N. Radiation and immunotherapy: a synergistic combination. *J. Clin. Invest.* **2013**, *123*, 2756-2763.

[10] Suneja, G.; Poorvu, P. D.; Hill-Kayser, C.; Lustig, R. A. Acute toxicity of proton beam radiation for pediatric central nervous system malignancies. *Pediatr. Blood Cancer* **2013**, *60*, 1431-1436.

[11] Kumar, A.; Cascarini, L.; McCaul, J. A.; Kerawala, C. J.; Coombes, D.; Godden, D.; Brennan, P. A. How should we manage oral leukoplakia? *Br. J. Oral Maxillofac. Surg.* **2013**, *51*, 377-383.

[12] Milovanovic, J.; Djukic, V.; Milovanovic, A.; Jotic, A.; Banko, B.; Jesic, S.; Babic, B.; Trivic, A.; Artiko, V.; Petrovic, M.; Stankovic, P. Clinical outcome of early glottic carcinoma in Serbia. *Auris Nasus Larynx* **2013**, *40*, 394-399.

[13] Moore, E. J.; Hinni, M. L. Critical Review: Transoral Laser Microsurgery and Robotic-Assisted Surgery for Oropharynx Cancer Including Human Papillomavirus-Related Cancer. *Int. J. Radiat. Oncol. Biol. Phys.* **2013**, *85*, 1163-1167.

[14] No, D.; Osterberg, E. C.; Otto, B.; Naftali, I.; Choi, B. Evaluation of continence following 532nm laser prostatectomy for patients previously treated with radiation therapy or brachytherapy. *Lasers Surg. Med.* **2013**, *45*, 358-361.

[15] Rosch, T. Progress in endoscopy: areas of current interest and topics to watch out for. *Endoscopy* **2012**, *44*, 1148-1157.

[16] Stummer, W.; Pichlmeier, U.; Meinel, T.; Wiestler, O. D.; Zanella, F.; Reulen, H.-J. r. Fluorescence-guided surgery with 5-aminolevulinic acid for resection of

malignant glioma: a randomised controlled multicentre phase III trial. *The Lancet Oncology* **2006**, *7*, 392-401.
[17] Troyan, S.; Kianzad, V.; Gibbs-Strauss, S.; Gioux, S.; Matsui, A.; Oketokoun, R.; Ngo, L.; Khamene, A.; Azar, F.; Frangioni, J. The FLARE Intraoperative Near-Infrared Fluorescence Imaging System: A First-in-Human Clinical Trial in Breast Cancer Sentinel Lymph Node Mapping. *Annals of Surgical Oncology* **2009**, *16*, 2943-2952.
[18] De Beer, E. L.; Bottone, A. E.; Voest, E. E. Doxorubicin and mechanical performance of cardiac trabeculae after acute and chronic treatment: a review. *European Journal of Pharmacology* **2001**, *415*, 1-11.
[19] Joseph, M. M. A., S. R. ;George, S. K. ;Pillai, K. R. ;Mini, S. ;Sreelekha, T. T. . Galactoxyloglucan-Modified Nanocarriers of Doxorubicin for Improved Tumor-Targeted Drug Delivery with Minimal Toxicity. *Journal of Biomedical Nanotechnology* **2014**, *10*, 3253-3268.
[20] Keizer, H. G.; Pinedo, H. M.; Schuurhuis, G. J.; Joenje, H. Doxorubicin (adriamycin): A critical review of free radical-dependent mechanisms of cytotoxicity. *Pharmacology & Therapeutics* **1990**, *47*, 219-231.
[21] Fagard, R.; Metelev, V.; Souissi, I. s.; Baran-Marszak, F. STAT3 inhibitors for cancer therapy: Have all roads been explored? *JAK-STAT* **2013**, *2*, e22882.
[22] Turkson, J. J., R. STAT proteins: novel molecular targets for cancer drug discovery. *Oncogene* **2000**, *19*, 6613-6626.
[23] Zhang, X.; Yue, P.; Page, B. D. G.; Li, T.; Zhao, W.; Namanja, A. T.; Paladino, D.; Zhao, J.; Chen, Y.; Gunning, P. T.; Turkson, J. Orally bioavailable small-molecule inhibitor of transcription factor Stat3 regresses human breast and lung cancer xenografts. *Proceedings of the National Academy of Sciences* **2012**, *109*, 9623-9628.
[24] Davis, M. E.; Chen, Z.; Shin, D. M. Nanoparticle therapeutics: an emerging treatment modality for cancer. *Nature Reviews Drug Discovery* **2008**, *7*, 771-782.
[25] Vyas, D. C., P. ;Saadeh, Y. ;Vyas, A. . The Role of Nanotechnology in Gastrointestinal Cancer. *Journal of Biomedical Nanotechnology* **2014**, *10*, 3204-3218.
[26] Brown, S. B.; Brown, E. A.; Walker, I. The present and future role of photodynamic therapy in cancer treatment. *The Lancet Oncology* **2004**, *5*, 497-508.
[27] Buinauskaite, E.; Maciulaitis, R.; Buinauskiene, J.; Valiukeviciene, S. Topical photodynamic therapy of actinic keratoses with 5-aminolevulinic acid: Randomized controlled trial with six months follow-up. *Journal of Dermatological Treatment* **2014**, *25*, 519-522.
[28] Casie Chetty, N.; Hemmant, B.; Skellett, A.-M. Periocular photodynamic therapy for squamous intra-epidermal carcinoma. *Journal of Dermatological Treatment* **2014**, *25*, 516-518.
[29] Gupta, A.; Avci, P.; Sadasivam, M.; Chandran, R.; Parizotto, N.; Vecchio, D.; de Melo, W.; Dai, T. H.; Chiang, L. Y.; Hamblin, M. R. Shining light on nanotechnology to help repair and regeneration. *Biotechnol. Adv.* **2012**, *31*, 607-631.
[30] Hopper, C. Photodynamic therapy: a clinical reality in the treatment of cancer. *The Lancet Oncology* **2000**, *1*, 212-219.
[31] Kubler, A. C. Photodynamic therapy. *Medical Laser Application* **2005**, *20*, 37-45.
[32] Dougherty, T. J.; Gomer, C. J.; Henderson, B. W.; Jori, G.; Kessel, D.; Korbelik, M.; Moan, J.; Peng, Q. Photodynamic therapy. *J. Natl. Cancer Inst.* **1998**, *90*, 889-905.

[33] Dolmans, D. E. J. G. J.; Fukumura, D.; Jain, R. K. Photodynamic therapy for cancer. *Nat Rev Cancer* **2003**, *3*, 380-387.
[34] Vrouenraets, M. B. V., G. W. M. ;Snow, G. B. ;van Dongen, Gams Basic principles, applications in oncology and improved selectivity of photodynamic therapy. *Anticancer Research* **2003**, *23*, 505-522.
[35] Wilson, B. C. Photodynamic therapy for cancer: Principles. *Canadian Journal of Gastroenterology & Hepatology* **2002**, *16*, 393 - 396.
[36] Shirasu, N.; Nam, S. O.; Kuroki, M. Tumor-targeted Photodynamic Therapy. *Anticancer Research* **2013**, *33*, 2823-2831.
[37] Lim, C.-K.; Heo, J.; Shin, S.; Jeong, K.; Seo, Y. H.; Jang, W.-D.; Park, C. R.; Park, S. Y.; Kim, S.; Kwon, I. C. Nanophotosensitizers toward advanced photodynamic therapy of Cancer. *Cancer Letters* **2013**, *334*, 176-187.
[38] Agostinis, P.; Berg, K.; Cengel, K. A.; Foster, T. H.; Girotti, A. W.; Gollnick, S. O.; Hahn, S. M.; Hamblin, M. R.; Juzeniene, A.; Kessel, D.; Korbelik, M.; Moan, J.; Mroz, P.; Nowis, D.; Piette, J.; Wilson, B. C.; Golab, J. Photodynamic Therapy of Cancer: An Update. *Ca-a Cancer Journal for Clinicians* **2011**, *61*, 250-281.
[39] Cheng, Y. H.; Cheng, H.; Jiang, C. X.; Qiu, X. F.; Wang, K. K.; Huan, W.; Yuan, A.; Wu, J. H.; Hu, Y. Q. Perfluorocarbon nanoparticles enhance reactive oxygen levels and tumour growth inhibition in photodynamic therapy. *Nature Communications* **2015**, *6*, 8785.
[40] Huang, Z.; Xu, H. P.; Meyers, A. D.; Musani, A. I.; Wang, L. W.; Tagg, R.; Barqawi, A. B.; Chen, Y. K. Photodynamic therapy for treatment of solid tumors - Potential and technical challenges. *Technology in Cancer Research & Treatment* **2008**, *7*, 309-320.
[41] Lee, K. L.; Carpenter, B. L.; Wen, A. M.; Ghiladi, R. A.; Steinmetz, N. F. High Aspect Ratio Nanotubes Formed by Tobacco Mosaic Virus for Delivery of Photodynamic Agents Targeting Melanoma. *Acs Biomaterials Science & Engineering* **2016**, *2*, 838-844.
[42] Wen, A. M.; Lee, K. L.; Cao, P. F.; Pangilinan, K.; Carpenter, B. L.; Lam, P.; Veliz, F. A.; Ghiladi, R. A.; Advincula, R. C.; Steinmetz, N. F. Utilizing Viral Nanoparticle/Dendron Hybrid Conjugates in Photodynamic Therapy for Dual Delivery to Macrophages and Cancer Cells. *Bioconjugate Chemistry* **2016**, *27*, 1227-1235.
[43] Chen, J.-Y.; Lee, Y.-M.; Zhao, D.; Mak, N.-K.; Wong, R. N.-S.; Chan, W.-H.; Cheung, N.-H. Quantum Dot-mediated Photoproduction of Reactive Oxygen Species for Cancer Cell Annihilation. *Photochemistry and Photobiology* **2010**, *86*, 431-437.
[44] Chou, K. L.; Meng, H.; Cen, Y.; Li, L.; Chen, J. Y. Dopamine-quantum dot conjugate: a new kind of photosensitizers for photodynamic therapy of cancers. *J. Nanopart. Res.* **2013**, *15*, 9.
[45] Huang, P.; Lin, J.; Wang, S.; Zhou, Z.; Li, Z.; Wang, Z.; Zhang, C.; Yue, X.; Niu, G.; Yang, M.; Cui, D.; Chen, X. Photosensitizer-conjugated silica-coated gold nanoclusters for fluorescence imaging-guided photodynamic therapy. *Biomaterials* **2013**, *34*, 4643-4654.
[46] Ito, S.; Miyoshi, N.; Degraff, W. G.; Nagashima, K.; Kirschenbaum, L. J.; Riesz, P. Enhancement of 5-Aminolevulinic acid-induced oxidative stress on two cancer cell lines by gold nanoparticles. *Free Radical Research* **2009**, *43*, 1214-1224.
[47] Vankayala, R.; Huang, Y.-K.; Kalluru, P.; Chiang, C.-S.; Hwang, K. C. First Demonstration of Gold Nanorods-Mediated Photodynamic Therapeutic Destruction of Tumors via Near Infra-Red

Light Activation. *Small* **2013**, *10*, 1612-1622.
[48] Perrier, M.; Gary-Bobo, M.; Lartigue, L.; Brevet, D.; Morere, A.; Garcia, M.; Maillard, P.; Raehm, L.; Guari, Y.; Larionova, J.; Durand, J. O.; Mongin, O.; Blanchard-Desce, M. Mannose-functionalized porous silica-coated magnetic nanoparticles for two-photon imaging or PDT of cancer cells. *J. Nanopart. Res.* **2013**, *15*, 17.
[49] Wang, F.; Chen, X. L.; Zhao, Z. X.; Tang, S. H.; Huang, X. Q.; Lin, C. H.; Cai, C. B.; Zheng, N. F. Synthesis of magnetic, fluorescent and mesoporous core-shell-structured nanoparticles for imaging, targeting and photodynamic therapy. *J. Mater. Chem.* **2011**, *21*, 11244-11252.
[50] Kim, S.; Ohulchanskyy, T. Y.; Pudavar, H. E.; Pandey, R. K.; Prasad, P. N. Organically modified silica nanoparticles co-encapsulating photosensitizing drug and aggregation-enhanced two-photon absorbing fluorescent dye aggregates for two-photon photodynamic therapy. *J. Am. Chem. Soc.* **2007**, *129*, 2669-2675.
[51] Tao, X.; Yang, Y.-J.; Liu, S.; Zheng, Y.-Z.; Fu, J.; Chen, J.-F. Poly(amidoamine) dendrimer-grafted porous hollow silica nanoparticles for enhanced intracellular photodynamic therapy. *Acta Biomaterialia* **2013**, *9*, 6431-6438.
[52] Zhao, Z. X.; Huang, Y. Z.; Shi, S. G.; Tang, S. H.; Li, D. H.; Chen, X. L. Cancer therapy improvement with mesoporous silica nanoparticles combining photodynamic and photothermal therapy. *Nanotechnology* **2014**, *25*, 285701.
[53] Ohulchanskyy, T. Y.; Roy, I.; Goswami, L. N.; Chen, Y.; Bergey, E. J.; Pandey, R. K.; Oseroff, A. R.; Prasad, P. N. Organically Modified Silica Nanoparticles with Covalently Incorporated Photosensitizer for Photodynamic Therapy of Cancer. *Nano Letters* **2007**, *7*, 2835-2842.
[54] Xue, C.; Wu, J.; Lan, F.; Liu, W.; Yang, X.; Zeng, F.; Xu, H. Nano Titanium Dioxide Induces the Generation of ROS and Potential Damage in HaCaT Cells Under UVA Irradiation. *Journal of Nanoscience and Nanotechnology* **2010**, *10*, 8500-8507.
[55] Ding, H.; Mora, R.; Gao, J.; Sumer, B. D. Characterization and Optimization of mTHPP Nanoparticles for Photodynamic Therapy of Head and Neck Cancer. *Otolaryngology -- Head and Neck Surgery* **2011**, *145*, 612-617.
[56] Kameyama, N. M., S. ;Itano, O. ;Ito, A. ;Konno, T. ;Arai, T. ;Ishihara, K. ;Ueda, M. ;Kitagawa, Y. Photodynamic Therapy Using an Anti-EGF Receptor Antibody Complexed with Verteporfin Nanoparticles: A Proof of Concept Study. *Cancer Biotherapy and Radiopharmaceuticals* **2011**, *26*, 697-704.
[57] Derycke, A. S. L.; de Witte, P. A. M. Liposomes for photodynamic therapy. *Adv. Drug Deliv. Rev.* **2004**, *56*, 17-30.
[58] Choi, K. H. C., C. W. ;Kim, C. H. ;Kim, D. H. ;Jeong, Y. I. ;Kang, D. H. . Effect of 5-Aminolevulinic Acid-Encapsulate Liposomes on Photodynamic Therapy in Human Cholangiocarcinoma Cells. *Journal of Nanoscience and Nanotechnology* **2014**, *14*, 5628-5632.
[59] Figueira, F. v.; M.R. Pereira, P.; Silva, S.; A.S. Cavaleiro, J.; P.C. Tome, J. Porphyrins and Phthalocyanines Decorated with Dendrimers: Synthesis and Biomedical Applications. *Current Organic Synthesis* **2014**, *11*, 110-126.
[60] Taratula, O.; Schumann, C.; Naleway, M. A.; Pang, A. J.; Chon, K. J.; Taratula, O. A Multifunctional Theranostic Platform Based on Phthalocyanine-Loaded Dendrimer for Image-Guided Drug Delivery and Photodynamic Therapy. *Molecular Pharmaceutics* **2013**, *10*, 3946-3958.
[61] Grimland, J. L.; Wu, C.; Ramoutar, R. R.; Brumaghim, J. L.; McNeill, J. Photosensitizer-doped conjugated polymer

nanoparticles with high cross-sections for one- and two-photon excitation. *Nanoscale* **2011**, *3*, 1451-1455.
[62] Shen, X.; Li, L.; Wu, H.; Yao, S. Q.; Xu, Q.-H. Photosensitizer-doped conjugated polymer nanoparticles for simultaneous two-photon imaging and two-photon photodynamic therapy in living cells. *Nanoscale* **2011**, *3*, 5140-5146.
[63] Zhang, Y.; Pang, L.; Ma, C.; Tu, Q.; Zhang, R.; Saeed, E.; Mahmoud, A. E.; Wang, J. Small Molecule-Initiated Light-Activated Semiconducting Polymer Dots: An Integrated Nanoplatform for Targeted Photodynamic Therapy and Imaging of Cancer Cells. *Analytical Chemistry* **2014**, *86*, 3092-3099.
[64] Feng, Z. Y.; Tao, P.; Zou, L.; Gao, P. L.; Liu, Y.; Liu, X.; Wang, H.; Liu, S. J.; Dong, Q. C.; Li, J.; Xu, B. S.; Huang, W.; Wong, W. Y.; Zhao, Q. Hyperbranched Phosphorescent Conjugated Polymer Dots with Iridium(III) Complex as the Core for Hypoxia Imaging and Photodynamic Therapy. *ACS Appl. Mater. Interfaces* **2017**, *9*, 28319-28330.
[65] Yang, T.; Liu, L.; Deng, Y. B.; Guo, Z. Q.; Zhang, G. B.; Ge, Z. S.; Ke, H. T.; Chen, H. B. Ultrastable Near-Infrared Conjugated-Polymer Nanoparticles for Dually Photoactive Tumor Inhibition. *Adv. Mater.* **2017**, *29*, 9.
[66] Kim, C.; Kim, S. Y.; Lim, Y. T.; Lee, T. S. Synthesis of conjugated polymer nanoparticles with core-shell structure for cell imaging and photodynamic cancer therapy. *Macromol. Res.* **2017**, *25*, 572-577.
[67] Feng, G.; Fang, Y.; Liu, J.; Geng, J.; Ding, D.; Liu, B. Multifunctional Conjugated Polymer Nanoparticles for Image-Guided Photodynamic and Photothermal Therapy. *Small* **2017**, *13*, 12.
[68] Haupt, S.; Lazar, I.; Weitman, H.; Shav-Tal, Y.; Ehrenberg, B. FRET energy transfer via Pdots improves the efficiency of photodynamic therapy and leads to rapid cell death. *J. Photochem. Photobiol. B-Biol.* **2016**, *164*, 123-131.
[69] Zhou, X. B.; Liang, H.; Jiang, P. F.; Zhang, K. Y.; Liu, S. J.; Yang, T. S.; Zhao, Q.; Yang, L. J.; Lv, W.; Yu, Q.; Huang, W. Multifunctional Phosphorescent Conjugated Polymer Dots for Hypoxia Imaging and Photodynamic Therapy of Cancer Cells. *Adv. Sci.* **2016**, *3*, 12.
[70] Shen, X. Q.; Li, S.; Li, L.; Yao, S. Q.; Xu, Q. H. Highly Efficient, Conjugated-Polymer-Based Nano-Photosensitizers for Selectively Targeted Two-Photon Photodynamic Therapy and Imaging of Cancer Cells. *Chem.-Eur. J.* **2015**, *21*, 2214-2221.
[71] Hu, Z.; Gesquiere, A. J. PCBM concentration dependent morphology of P3HT in composite P3HT/PCBM nanoparticles. *Chemical Physics Letters* **2009**, *476*, 51-55.
[72] Hu, Z.; Gesquiere, A. J. Charge Trapping and Storage by Composite P3HT/PC60BM Nanoparticles Investigated by Fluorescence-Voltage/Single Particle Spectroscopy. *J. Am. Chem. Soc.* **2011**, *133*, 20850-20856.
[73] Hu, Z.; Tenery, D.; Bonner, M. S.; Gesquiere, A. J. Correlation between spectroscopic and morphological properties of composite P3HT/PCBM nanoparticles studied by single particle spectroscopy. *Journal of Luminescence* **2010**, *130*, 771-780.
[74] Tenery, D.; Gesquiere, A. J. Effect of PCBM Concentration on Photoluminescence Properties of Composite MEH-PPV/PCBM Nanoparticles Investigated by a Franck-Condon Analysis of Single-Particle Emission Spectra. *Chemphyschem* **2009**, *10*, 2449-2457.
[75] Tenery, D.; Gesquiere, A. J. Interplay between fluorescence and morphology in composite MEH-PPV/PCBM nanoparticles studied at the single particle level. *Chemical Physics* **2009**, *365*, 138-143.

[76] Tenery, D.; Worden, J. G.; Hu, Z.; Gesquiere, A. J. Single particle spectroscopy on composite MEH-PPV/PCBM nanoparticles. *Journal of Luminescence* **2009**, *129*, 423-429.
[77] Yu, J.; Lammi, R.; Gesquiere, A. J.; Barbara, P. F. Singlet-triplet and triplet-triplet interactions in conjugated polymer single molecules. *Journal of Physical Chemistry B* **2005**, *109*, 10025-10034.
[78] Wu, C.; Hansen, S. J.; Hou, Q.; Yu, J.; Zeigler, M.; Jin, Y.; Burnham, D. R.; McNeill, J. D.; Olson, J. M.; Chiu, D. T. Design of Highly Emissive Polymer Dot Bioconjugates for In Vivo Tumor Targeting. *Angewandte Chemie-International Edition* **2011**, *50*, 3430-3434.
[79] Sariciftci, N. S.; Smilowitz, L.; Heeger, A. J.; Wudl, F. Photoinduced electron transfer from a conducting polymer to buckminsterfullerene. *Science* **1992**, *258*, 1474-1476.
[80] Sperandio, F. F.; Sharma, S. K.; Wang, M.; Jeon, S.; Huang, Y. Y.; Dai, T. H.; Nayka, S.; de Sousa, S.; Chiang, L. Y.; Hamblin, M. R. Photoinduced electron-transfer mechanisms for radical-enhanced photodynamic therapy mediated by water-soluble decacationic C-70 and C84O2 Fullerene Derivatives. *Nanomed.-Nanotechnol. Biol. Med.* **2013**, *9*, 570-579.
[81] Fan, J. Q.; Fang, G.; Zeng, F.; Wang, X. D.; Wu, S. Z. Water-Dispersible Fullerene Aggregates as a Targeted Anticancer Prodrug with both Chemo- and Photodynamic Therapeutic Actions. *Small* **2013**, *9*, 613-621.
[82] Grynyuk, I.; Grebinyk, S.; Prylutska, S.; Mykhailova, A.; Franskevich, D.; Matyshevska, O.; Schutze, C.; Ritter, U. Photoexcited fullerene C-60 disturbs prooxidant-antioxidant balance in leukemic L1210 cells. *Materialwiss. Werkstofftech.* **2013**, *44*, 139-143.
[83] Liu, X. M.; Zheng, M.; Kong, X. G.; Zhang, Y. L.; Zeng, Q. H.; Sun, Z. C.; Buma, W. J.; Zhang, H. Separately doped upconversion-C-60 nanoplatform for NIR imaging-guided photodynamic therapy of cancer cells. *Chem. Commun.* **2013**, *49*, 3224-3226.
[84] Trpkovic, A.; Todorovic-Markovic, B.; Trajkovic, V. Toxicity of pristine versus functionalized fullerenes: mechanisms of cell damage and the role of oxidative stress. *Arch. Toxicol.* **2012**, *86*, 1809-1827.
[85] Chen, Z. Y.; Ma, L. J.; Liu, Y.; Chen, C. Y. Applications of Functionalized Fullerenes in Tumor Theranostics. *Theranostics* **2012**, *2*, 238-250.
[86] Gao, H. J.; Shi, W. D.; Freund, L. B. Mechanics of receptor-mediated endocytosis. *Proc. Natl. Acad. Sci. U. S. A.* **2005**, *102*, 9469-9474.
[87] Lerch, S.; Dass, M.; Musyanovych, A.; Landfester, K.; Mailander, V. Polymeric nanoparticles of different sizes overcome the cell membrane barrier. *Eur. J. Pharm. Biopharm.* **2013**, *84*, 265-274.
[88] Tang, L.; Gabrielson, N. P.; Uckun, F. M.; Fan, T. M.; Cheng, J. J. Size-Dependent Tumor Penetration and in Vivo Efficacy of Monodisperse Drug-Silica Nanoconjugates. *Molecular Pharmaceutics* **2013**, *10*, 883-892.
[89] Park, S. H.; Roy, A.; Beaupré, S.; Cho, S.; Coates, N.; Moon, J. S.; Moses, D.; Leclerc, M.; Lee, K.; Heeger, A. J. Bulk heterojunction solar cells with internal quantum efficiency approaching 100%. *Nature Photonics* **2009**, *3*, 297-302.
[90] Doshi, M.; Treglown, K.; Copik, A.; Gesquiere, A. J. Composite Conjugated Polymer/Fullerene Nanoparticles as Sensitizers in Photodynamic Therapy for Cancer. *BioNanoScience* **2014**, *4*, 15-26.
[91] Ross, J. F.; Chaudhuri, P. K.; Ratnam, M. Differential regulation of folate receptor isoforms in normal and malignant tissues in vivo and in established cell lines. Physiologic and clinical implications. *Cancer* **1994**, *73*, 2432-2443.

[92] Parker, N.; Turk, M. J.; Westrick, E.; Lewis, J. D.; Low, P. S.; Leamon, C. P. Folate receptor expression in carcinomas and normal tissues determined by a quantitative radioligand binding assay. *Analytical Biochemistry* **2005**, *338*, 284-293.
[93] Zhang, Y.; Yang, M.; Portney, N. G.; Cui, D. X.; Budak, G.; Ozbay, E.; Ozkan, M.; Ozkan, C. S. Zeta potential: a surface electrical characteristic to probe the interaction of nanoparticles with normal and cancer human breast epithelial cells. *Biomed. Microdevices* **2008**, *10*, 321-328.
[94] Gratton, S. E. A.; Ropp, P. A.; Pohlhaus, P. D.; Luft, J. C.; Madden, V. J.; Napier, M. E.; DeSimone, J. M. The effect of particle design on cellular internalization pathways. *Proc. Natl. Acad. Sci. U. S. A.* **2008**, *105*, 11613-11618.
[95] Huhn, D.; Kantner, K.; Geidel, C.; Brandholt, S.; De Cock, I.; Soenen, S. J. H.; Gil, P. R.; Montenegro, J. M.; Braeckmans, K.; Mullen, K.; Nienhaus, G. U.; Klapper, M.; Parak, W. J. Polymer-Coated Nanoparticles Interacting with Proteins and Cells: Focusing on the Sign of the Net Charge. *ACS Nano* **2013**, *7*, 3253-3263.
[96] Xu, P. S.; Van Kirk, E. A.; Zhan, Y. H.; Murdoch, W. J.; Radosz, M.; Shen, Y. Q. Targeted charge-reversal nanoparticles for nuclear drug delivery. *Angewandte Chemie-International Edition* **2007**, *46*, 4999-5002.
[97] Valko, M.; Rhodes, C. J.; Moncol, J.; Izakovic, M.; Mazur, M. Free radicals, metals and antioxidants in oxidative stress-induced cancer. *Chem.-Biol. Interact.* **2006**, *160*, 1-40.
[98] Toffoli, G.; Cernigoi, C.; Russo, A.; Gallo, A.; Bagnoli, M.; Boiocchi, M. Overexpression of folate binding protein in ovarian cancers. *Int. J. Cancer* **1997**, *74*, 193-198.
[99] Schumacker, P. T. Reactive oxygen species in cancer cells: Live by the sword, die by the sword. *Cancer Cell* **2006**, *10*, 175-176.
[100] Lee, J.; Twomey, M.; Machado, C.; Gomez, G.; Doshi, M.; Gesquiere, A. J.; Moon, J. H. Caveolae-Mediated Endocytosis of Conjugated Polymer Nanoparticles. *Macromolecular Bioscience* **2013**, *13*, 913-920.
[101] Kim, J.-S.; Yoon, T.-J.; Yu, K.-N.; Noh, M. S.; Woo, M.; Kim, B.-G.; Lee, K.-H.; Sohn, B.-H.; Park, S.-B.; Lee, J.-K.; Cho, M.-H. Cellular uptake of magnetic nanoparticle is mediated through energy-dependent endocytosis in A549 cells. *J Vet Sci* **2006**, *7*, 321-326.
[102] Fretz, M. M.; Koning, G. A.; Mastrobattista, A.; Jiskoot, W.; Storm, G. OVCAR-3 cells internalize TAT-peptide modified liposomes by endocytosis. *Biochimica Et Biophysica Acta-Biomembranes* **2004**, *1665*, 48-56.
[103] Doshi, M.; Copik, A.; Gesquiere, A. J. Development and characterization of conducting polymer nanoparticles for photodynamic therapy in vitro. *Photodiagnosis and Photodynamic Therapy* **2015**, *12*, 476-489.
[104] Houle, J.-M.; Strong, H. A. Duration of Skin Photosensitivity and Incidence of Photosensitivity Reactions After Administration of Verteporfin. *RETINA* **2002**, *22*, 691-697.
[105] Moriwaki, S.-I.; Misawa, J.; Yoshinari, Y.; Yamada, I.; Takigawa, M.; Tokura, Y. Analysis of photosensitivity in Japanese cancer-bearing patients receiving photodynamic therapy with porfimer sodium (PhotofrinTM). *Photodermatology, Photoimmunology & Photomedicine* **2001**, *17*, 241-243.
[106] van Dongen, G. A. M. S.; Visser, G. W. M.; Vrouenraets, M. B. Photosensitizer-antibody conjugates for detection and therapy of cancer. *Adv. Drug Deliv. Rev.* **2004**, *56*, 31-52.

[107] Weitman, S. D.; Lark, R. H.; Coney, L. R.; Fort, D. W.; Frasca, V.; Zurawski, V. R.; Kamen, B. A. Distribution of the Folate Receptor GP38 in Normal and Malignant Cell Lines and Tissues. *Cancer Research* **1992**, *52*, 3396-3401.

[108] Real, F. X.; Rettig, W. J.; Chesa, P. G.; Melamed, M. R.; Old, L. J.; Mendelsohn, J. Expression of Epidermal Growth Factor Receptor in Human Cultured Cells and Tissues: Relationship to Cell Lineage and Stage of Differentiation. *Cancer Research* **1986**, *46*, 4726-4731.

[109] Ahmed, N.; Salsman, V. S.; Yvon, E.; Louis, C. U.; Perlaky, L.; Wels, W. S.; Dishop, M. K.; Kleinerman, E. E.; Pule, M.; Rooney, C. M.; Heslop, H. E.; Gottschalk, S. Immunotherapy for Osteosarcoma: Genetic Modification of T cells Overcomes Low Levels of Tumor Antigen Expression. *Mol Ther* **2009**, *17*, 1779-1787.

[110] Subik, K.; Lee, J.-F.; Baxter, L.; Strzepek, T.; Costello, D.; Crowley, P.; Xing, L.; Hung, M.-C.; Bonfiglio, T.; Hicks, D. G.; Tang, P. The Expression Patterns of ER, PR, HER2, CK5/6, EGFR, Ki-67 and AR by Immunohistochemical Analysis in Breast Cancer Cell Lines. *Breast Cancer: Basic and Clinical Research* **2010**, *4*, 35-41.

[111] Doshi, M.; Krienke, M.; Khederzadeh, S.; Sanchez, H.; Copik, A.; Oyer, J.; Gesquiere, A. J. Conducting polymer nanoparticles for targeted cancer therapy. *RSC Advances* **2015**, *5*, 37943-37956.

[112] Antony, A. C. Folate Receptors. *Annual Review of Nutrition* **1996**, *16*, 501-521.

[113] Campbell, I. G.; Jones, T. A.; Foulkes, W. D.; Trowsdale, J. Folate-binding Protein Is a Marker for Ovarian Cancer. *Cancer Research* **1991**, *51*, 5329-5338.

[114] Sudimack, J.; Lee, R. J. Targeted drug delivery via the folate receptor. *Adv. Drug Deliv. Rev.* **2000**, *41*, 147-162.

[115] Scarano, W.; Duong, H. T. T.; Lu, H.; De Souza, P. L.; Stenzel, M. H. Folate Conjugation to Polymeric Micelles via Boronic Acid Ester to Deliver Platinum Drugs to Ovarian Cancer Cell Lines. *Biomacromolecules* **2013**, *14*, 962-975.

[116] Garinchesa, P. C., I. ;Saigo, P. E. ;Lewis, J. L. ;Old, L. J. ;Rettig, W. J. . Trophoblast and Ovarian-Cancer Antigen-LK26 -Sensitivity and Specificity in Immunopathology and Molecular-Identification as a Folate-Binding Protein. *American Journal of Pathology* **1993**, *142*, 557-567.

[117] Bharali, D. J.; Lucey, D. W.; Jayakumar, H.; Pudavar, H. E.; Prasad, P. N. Folate-Receptor-Mediated Delivery of InP Quantum Dots for Bioimaging Using Confocal and Two-Photon Microscopy. *J. Am. Chem. Soc.* **2005**, *127*, 11364-11371.

[118] Choi, H.; Choi, S. R.; Zhou, R.; Kung, H. F.; Chen, I. W. Iron oxide nanoparticles as magnetic resonance contrast agent for tumor imaging via folate receptor-targeted delivery1. *Academic Radiology* **2004**, *11*, 996-1004.

[119] Hwa Kim, S.; Hoon Jeong, J.; Joe, C. O.; Gwan Park, T. Folate receptor mediated intracellular protein delivery using PLL-PEG-FOL conjugate. *Journal of Controlled Release* **2005**, *103*, 625-634.

[120] Koyakutty, M.; Seby, J.; Deepa, T.; Sonali, S.; Deepthy, M.; Shantikumar, N. Bio-conjugated luminescent quantum dots of doped ZnS: a cyto-friendly system for targeted cancer imaging. *Nanotechnology* **2009**, *20*, 065102.

[121] Lee, D.; Lockey, R.; Mohapatra, S. Folate Receptor-Mediated Cancer Cell Specific Gene Delivery Using Folic Acid-Conjugated Oligochitosans. *Journal of Nanoscience and Nanotechnology* **2006**, *6*, 2860-2866.

[122] Doshi, M.; Treglown, K.; Copik, A.; Gesquiere, A. Composite Conjugated Polymer/Fullerene Nanoparticles as

Sensitizers in Photodynamic Therapy for Cancer. *BioNanoScience* **2014**, *4*, 15-26.
[123] Setua, S.; Menon, D.; Asok, A.; Nair, S.; Koyakutty, M. Folate receptor targeted, rare-earth oxide nanocrystals for bi-modal fluorescence and magnetic imaging of cancer cells. *Biomaterials* **2010**, *31*, 714-729.
[124] Tavassolian, F.; Kamalinia, G.; Rouhani, H.; Amini, M.; Ostad, S. N.; Khoshayand, M. R.; Atyabi, F.; Tehrani, M. R.; Dinarvand, R. Targeted poly (L-Y-glutamyl glutamine) nanoparticles of docetaxel against folate over-expressed breast cancer cells. *International Journal of Pharmaceutics* **2014**, *467*, 123-138.
[125] Yoo, H. S.; Park, T. G. Folate-receptor-targeted delivery of doxorubicin nano-aggregates stabilized by doxorubicin-PEG-folate conjugate. *Journal of Controlled Release* **2004**, *100*, 247-256.

